Journal of proteome research

Article

pubs.acs.org/jpr



# Proteomic Quantification and Site-Mapping of *S*-Nitrosylated Proteins Using Isobaric iodoTMT Reagents

Zhe Qu,[†,§] Fanjun Meng,[†,§,&] Ryan D. Bomgarden,[○] Rosa I. Viner,[∥] Jilong Li,[⊥] John C. Rogers,[○] Jianlin Cheng,[⊥] C. Michael Greenlief,[#] Jiankun Cui,[†,§,●] Dennis B. Lubahn,[‡] Grace Y. Sun,[†,‡,§] and Zezong Gu*[,†,§,●]

[†]Department of Pathology and Anatomical Sciences, [‡]Department of Biochemistry, and [§]Center for Translational Neuroscience, University of Missouri School of Medicine, Columbia, Missouri, United States

[⊥]Department of Computer Science, Informatics Institute, University of Missouri College of Engineering, Columbia, Missouri, United States

[#]Department of Chemistry, University of Missouri College of Arts and Science, Columbia, Missouri, United States

[●]Harry S. Truman Veterans Hospital, Columbia, Missouri, United States

[○]Pierce Protein Research, Thermo Fisher Scientific, Rockford, Illinois, United States

[∥]Division of Manufacturing, Thermo Fisher Scientific, San Jose, California, United States

Supporting Information

**ABSTRACT:** *S*-Nitrosylation is a redox-based protein post-translational modification in response to nitric oxide signaling and is involved in a wide range of biological processes. Detection and quantification of protein *S*-nitrosylation have been challenging tasks due to instability and low abundance of the modification. Many studies have used mass spectrometry (MS)-based methods with different thiol-reactive reagents to label and identify proteins with *S*-nitrosylated cysteine (SNO-Cys). In this study, we developed a novel iodoTMT switch assay (ISA) using an isobaric set of thiol-reactive iodoTMT-sixplex reagents to specifically detect and quantify protein *S*-nitrosylation. Irreversible labeling of SNO-Cys with the iodoTMTsixplex reagents enables immune-affinity detection of *S*-nitrosylated proteins, enrichment of iodoTMT-labeled peptides by anti-TMT resin, and importantly, unambiguous modification site-mapping and multiplex quantification by liquid chromatography−tandem MS. Additionally, we significantly improved anti-TMT peptide enrichment efficiency by competitive elution. Using ISA, we identified a set of SNO-Cys sites responding to lipopolysaccharide (LPS) stimulation in murine BV-2 microglial cells and revealed effects of *S*-allyl cysteine from garlic on LPS-induced protein *S*-nitrosylation in antioxidative signaling and mitochondrial metabolic pathways. ISA proved to be an effective proteomic approach for quantitative analysis of *S*-nitrosylation in complex samples and will facilitate the elucidation of molecular mechanisms of nitrosative stress in disease.

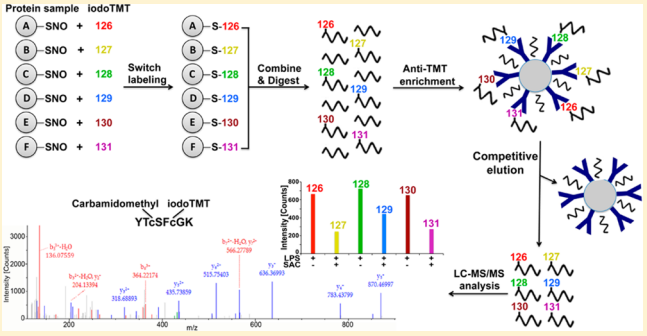


**KEYWORDS:** *iodoTMTsixplex, quantitative proteomics, S-nitrosylation, microglia, S-allyl cysteine*

## INTRODUCTION

Nitric oxide (NO) is a pleiotropic signaling molecule produced endogenously by NO synthases in diverse biological systems. *S*-Nitrosylation is the addition of a NO group to a specific cysteine (Cys) residue of a protein to form a *S*-nitrosothiol. This prototypic, redox-based post-translational protein modification process has been increasingly recognized as a key cellular and molecular mechanism for NO signaling and plays an important role in physiological conditions and in diseases such as diabetes, asthma, heart failure, cancer, and neurodegenerative disorders.[1−3] *S*-Nitrosylation of critical Cys residues on specific proteins regulates their activities and has been demonstrated in protein misfolding resulting in interference of normal cellular functions.[3]

In order to investigate mechanisms underlying NO signaling, a number of methods have been established for identifying *S*-nitrosylated proteins (SNO-proteins) and mapping their *S*-nitrosylated cysteine (SNO-Cys) sites. The biotin switch technique (BST) developed by Jaffrey et al.[4] is the most commonly used approach to detect SNO-proteins *in vivo*. It involves first blocking free thiols with a sulfhydryl-reactive reagent, such as *S*-methyl methanethiosulfonate (MMTS), then selectively reducing the *S*-nitrosothiols with ascorbate, and labeling with *N*-[6-(biotinamido)hexyl]-3′-(2′-pyridyldithio) propionamide (biotin-HPDP). The biotinylated SNO-proteins

**Received:** November 29, 2013
**Published:** June 2, 2014

   dx.doi.org/10.1021/pr401179v | *J. Proteome Res.* 2014, 13, 3200−3211

can be enriched via avidin-agarose affinity capture, and then proteins of interest are detected by immunoblotting. Despite its popularity, this method is relatively low-throughput, and it is difficult to locate the modification sites. Additionally, the biotin affinity enrichment may introduce false positive signals due to the existence of endogenous biotin-like molecules. To specifically assess SNO-Cys modification status and increase the throughput of detection, several mass spectrometry (MS)-based methods have been developed by modifying the BST protocol, including SNO-Cys site identification (SNOSID), *S*-nitrosothiol resin-assisted capture (SNO-RAC), *S*-alkylating labeling strategy, and cysTMT switch assay.[5−8] However, none of these modified BST methods are able to achieve all of the following features desired for comprehensive characterization of SNO-Cys modification: a simple, robust workflow for SNO-protein identification, an irreversible thiol linkage for effective peptide digestion and for unambiguous SNO-Cys mapping, as well as sample multiplexing for increased throughput and relative quantification of SNO-proteins under various conditions.

In this study, we present a novel MS-based modified BST, the iodoTMT switch assay (ISA), using Cys thiol-reactive iodoacetyl tandem mass tag (iodoTMT) sixplex reagents to identify and quantify protein *S*-nitrosylation. With a simple workflow, ISA accomplishes irreversible labeling of SNO-Cys sites, *S*-nitrosylated peptide (SNO-peptide) enrichment using high affinity anti-TMT chromatography with competitive elution, and multiplex quantification of protein *S*-nitrosylation via six unique TMT mass reporter ions. Notably, this workflow is capable of detection and quantification of SNO-Cys modifications under physiological and pathological conditions. In this study, we applied this approach to the investigation of protein *S*-nitrosylation in a neuroinflammation model——endotoxin lipopolysaccharide (LPS)-stimulated immortalized murine BV-2 microglial cells—representing a convergent nitrosative stress and neuroinflammatory response in the pathogenesis of age-associated neurodegenerative diseases.[9,10] We further evaluated the effects of *S*-allyl cysteine (SAC), an active nutritional compound of aged garlic extract (AGE), on LPS-stimulated *S*-nitrosylation in BV-2 cells.

## MATERIALS AND METHODS

### Materials

The iodoTMTsixplex reagents, anti-TMT antibody, immobilized anti-TMT antibody resin, bicinchoninic acid (BCA) protein assay kit, C18 tips, and primary antibodies for protein validation were obtained from Thermo Fisher Scientific (Rockford, IL). Fetal bovine serum (FBS) was purchased from Atlanta Biologicals, Inc. (Lawrenceville, GA). Sep-Pak tC18 1 cc Vac Cartridges were purchased from Waters (Dublin, Ireland). Amersham ECL Prime Western Blotting Detection Reagent was purchased from GE Healthcare (Buckinghamshire, UK). Trypsin (modified, sequencing grade) was obtained from Promega (Madison, WI). Dulbecco's modified Eagle's medium (DMEM), penicillin-streptomycin, and L-glutamine were obtained from Gibco (Grand Island, NY). All other reagents including SAC (a garlic active component) were from Sigma-Aldrich (St. Louis, MO). The purity and stability of SAC were validated prior to use through the Nutrition Core of the Center for Botanical Interaction Studies at the University of Missouri.

### Cell Culture and Treatment

The immortalized murine BV-2 microglial cells were cultured in DMEM containing 5% (v/v) heat-inactivated FBS, 25 U/mL penicillin, and 25 $\mu$g/mL streptomycin at 37 °C in a saturated humidity atmosphere containing 95% (v/v) air and 5% (v/v) $CO_2$. Cells were plated at a density of $1 \times 10^5$/mL medium in 35 mm or 100 mm plates and grown to 70% confluence prior to testing. BV-2 cells were starved for 4 h in FBS-free DMEM (without phenol red) and then exposed to 100 ng/mL LPS for 16 h in the presence or absence of 5 mM SAC or 0.5 mM *N*-$\omega$-nitro-L-arginine methyl ester hydrochloride (L-NAME).

### Measurement of NO

Griess assay was performed to measure the production of NO. After LPS stimulation, conditioned medium was collected and mixed with an equal volume of Griess reagent [1% (w/v) sulfanilamide and 0.1% (w/v) *N*-(1-naphthyl) ethylenediamide in 5% (v/v) phosphoric acid]. After a 10 min incubation at room temperature (RT), absorbance was read at 543 nm using a BioTek Synergy-4 microplate reader (BioTek Instruments, Inc., Winooski, VT). To calculate NO concentration, a series of sodium nitrite dilutions (0−100 $\mu$M) was used to generate a nitrite standard reference curve.[11]

### MTT Cell Viability Assay

Cell viability was determined by MTT assay as previously described with modifications.[12] After treatment, 0.5 mg/mL 3-(4,5-dimethylthiazol-2-yl)-2,5-diphenyl-2*H*-tetrazolium bromide (MTT) was added to the cell culture. After incubation at 37 °C for 4 h, the formed formazan crystals were collected and dissolved in dimethyl sulfoxide (DMSO). The absorbance at 540 nm was read using the Synergy-4 microplate reader.

### Protein Sample Preparation

For *in vitro* *S*-nitrosylation, 400 $\mu$g of BV-2 cell lysates in HENTS buffer [250 mM HEPES-NaOH, pH 7.4, 1 mM EDTA, 0.1 mM neocuproine, 1% (v/v) Triton X-100, 0.1% (w/v) SDS, 1% (v/v) protease inhibitor cocktail] were exposed to a final concentration of 200 $\mu$M *S*-nitrosocysteine (SNOC) for 30 min at RT in the dark. *In vivo* treated BV-2 cells were rinsed twice in cold phosphate-buffered saline followed by lysis in HENTS buffer. Protein concentrations were measured by BCA assay following the manufacturer's manual.

### iodoTMT Switch Labeling of SNO-Proteins

The iodoTMT labeling was conducted by modifying the BST method.[4] Free sulfhydryl groups in the protein sample were first blocked with 20 mM MMTS for 30 min at 50 °C with frequent vortexing in HEN (250 mM HEPES-NaOH, pH 7.4, 1 mM EDTA, 0.1 mM neocuproine) buffer containing 2.5% (w/v) SDS. To remove excess MMTS, proteins were precipitated using 4× volume of cold acetone for 30 min at −20 °C. Proteins were then redissolved in HEN buffer containing 1% (w/v) SDS and labeled with 1 mM iodoTMT reagent in the presence of 5 mM sodium ascorbate for 2 h at RT. All above procedures were performed with protection from light. For MS analysis, after acetone precipitation, iodoTMT-labeled proteins were redissolved with Tris-HCl, pH 8.0, containing 0.1% (w/v) SDS. Six different protein samples individually labeled by iodoTMTsixplex reagents were combined before tryptic digestion.


dx.doi.org/10.1021/pr401179v | J. Proteome Res. 2014, 13, 3200−3211

### In-Solution Tryptic Digestion and Anti-TMT Peptide Enrichment

The iodoTMT-labeled proteins were reduced with 10 mM dithiothreitol (DTT) at 55 °C for 1 h and then alkylated with 25 mM iodoacetamide at 37 °C for 1 h in the dark. After acetone precipitation, the protein pellet was resuspended with 50 mM ammonium bicarbonate containing 20 ng/μL trypsin and digested overnight at 37 °C. Undigested proteins were removed by centrifuge at 2500*g*, RT for 10 min. The peptides were then desalted with 50 mg Waters Sep-Pak tC18 columns and eluted with 50% (v/v) acetonitrile (ACN) and 0.1% (v/v) trifluoroacetic acid (TFA). A small portion of this unfractionated sample was retained for future analysis of the unenriched sample.

For peptide enrichment, the above samples were lyophilized and redissolved in 600 μL of TBS buffer (25 mM Tris-HCl, pH 7.5, 0.15 M NaCl). Typically, 100 μL of settled immobilized anti-TMT antibody resin is employed for enrichment of every 1 mg of *S*-nitrosylated sample. In our experiments, the peptide sample was incubated with 200 μL of settled anti-TMT antibody resin overnight at 4 °C with end-over-end rocking. After the supernatant was removed, the resin was washed three times with one column volume of TBS and three times with one column volume of Milli-Q water. Peptides were finally eluted with four column volumes of elution buffer [10 mM cis-2,6-dimethylpiperidine (2,6-DMPp)/500 mM tetraethylammonium bicarbonate (TEAB), pH 8.5].

### Protein Identification by Liquid Chromatography–Tandem MS (LC–MS/MS)

A EASY-nLC 1000 HPLC system and EASYSpray source (Thermo Scientific) with EASY-Spray PepMap RSLC C18 25 cm × 75 μm ID column (Thermo Scientific) were used to separate peptides with a 5–25% (v/v) ACN gradient in 0.1% (v/v) formic acid over 120 min at a flow rate of 300 nL/min. Samples were analyzed on Orbitrap Elite and LTQ Orbitrap XL mass spectrometers (Thermo Scientific) using top 15 Fourier transform (FT) MS/MS with higher-energy collision dissociation (HCD) or top 3/3 ion-trap collision-induced dissociation (CID)/FT HCD experiments.

Proteome Discoverer software version 1.4 (Thermo Scientific) was used to search MS/MS spectra against the Swiss-Prot mouse database using the SEQUEST HT or Mascot 2.3 search engines. Dynamic modifications included carbamidomethylation (C), iodoTMTsixplex (C), and methionine oxidation. Resulting peptide hits were filtered for a maximum 5% false discovery rate using the Percolator. The iodoTMTsixplex quantification method within Proteome Discoverer software was used to calculate the reporter ratios with a mass tolerance ±10 ppm.

### Surface Plasmon Resonance

Anti-TMT antibody affinity was determined using a TMT-derivatized CM5 chip on a BIACORE 3000 instrument (GE Healthcare). For competitive elution buffer scouting, anti-TMT antibody was first bound to TMT-derivatized surface followed by a timed injection of TMT analogue compounds.

### SDS-PAGE and Immunoblotting

For SDS-PAGE, 4× SDS sample buffer with 1% (v/v) 2-mercaptoethanol was added to the protein samples. Proteins were then resolved on 10%, 1 mm SDS-PAGE gels. For immunoblotting, proteins in SDS-PAGE gel were transferred to a nitrocellulose membrane. The membrane was first blocked in phosphate-buffered saline plus 0.1% (v/v) Tween-20 (PBST) containing 5% (w/v) nonfat milk at RT for 1 h followed by incubation with primary antibody in PBST at 4 °C overnight. After being washed three times with PBST, the membrane was incubated with secondary antibody (anti-mouse IgG-peroxidase antibody produced in goat or anti-rabbit IgG-peroxidase antibody produced in goat, Sigma) in PBST at RT for 1 h. Immuno-reactive bands were visualized using Amersham ECL Prime Western Blotting Detection Reagent and detected with LAS-4000 imaging system (Fujifilm).

### Statistical Analysis

Degree of freedom and *z* score for each iodoTMT modification site was calculated by a special Student's *t*-test, known as Welch's *t*-test.[13] We further used a *t*-distribution[14,15] implemented in the R statistical package to calculate the *p*-value based on degree of freedom and *z* score. *S*-Nitrosylation level change of a SNO-Cys was considered as significant if its fold change is greater than 1.3 and *p*-value is less than 0.05.

### Bioinformatics

Motif consensus sequences for protein *S*-nitrosylation was analyzed by the Motif-X algorithm.[16] SNO-proteins with significant *S*-nitrosylation level changes were subjected to functional annotation by Ingenuity Pathway Analysis (IPA; http://www.ingenuity.com) and the in-house MULTICOM-PDCN[17] software.

## RESULTS

### Detection of SNO-Proteins by iodoTMT Switch Labeling

iodoTMTsixplex reagents are commercially available and were used in the study to determine protein *S*-nitrosylation. Each isobaric iodoTMTsixplex reagent within a set has the same nominal mass and consists of a thiol-reactive iodoacetyl group, a MS-neutral spacer arm, and a MS/MS reporter. The chemical structure of iodoTMT-126 (one of the sixplex reagents; 126 refers to the mass of the reporter ion) is shown in Figure 1A. During MS/MS analysis to derive fragment ions and sequence information, the isobaric mass tags are cleaved generating reporter ions with unique *m*/*z* of 126–131. In ISA, after blocking free thiols in the proteins with MMTS, an iodoTMT reagent is used to irreversibly label nascent thiols generated by the selective reduction of SNO-Cys bonds by ascorbate (Figure 1B). The irreversibility of iodoTMT labeling was validated under our tested conditions (Supplemental Figure S1, Supporting Information). To test the specificity of iodoTMT labeling, BV-2 cell lysates were *S*-nitrosylated *in vitro* by exposure to a physiological NO donor SNOC (200 μM) and followed by labeling with iodoTMT-126. As shown in Figure 1C, iodoTMT-labeled samples showed much stronger signals than control conditions without SNOC and/or ascorbate on the anti-TMT immunoblot. To test the sensitivity of the iodoTMT labeling assay, BV-2 cell lysates were treated with different concentrations (10, 50, 100, 200 μM) of SNOC. After switch labeling with iodoTMT-126, SNO-protein signals in SNOC-treated samples exhibited a dose-dependent increase compared to the untreated control sample (Figure 1D). These results suggested that iodoTMT switch labeling is feasible and reliable for detecting SNO-proteins and is sensitive to as low as 10 μM SNOC treatment.

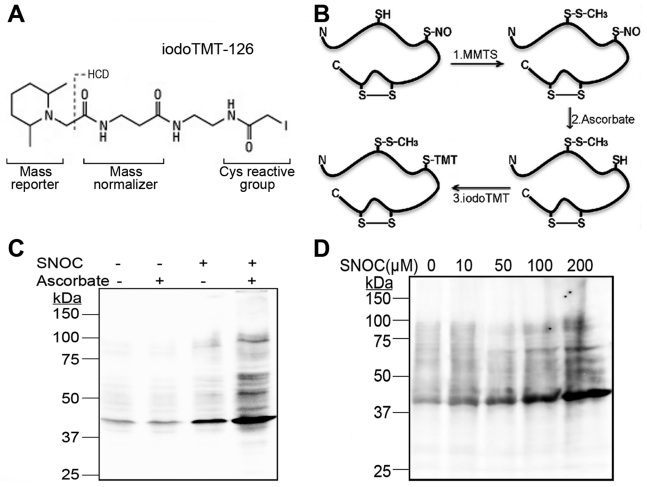


**Figure 1.** Detection of protein *S*-nitrosylation by iodoTMT switch labeling. (A) The chemical structure of iodoTMT-126 reagent. The iodoTMTsixplex reagents including iodoTMT-126 illustrated here consist of a Cys thiol-reactive iodoacetyl group, a mass normalizing spacer arm, and a mass reporter. MS/MS fragmentation site by HCD is indicated. (B) Reaction scheme for the labeling of SNO-protein by iodoTMT reagents. Free thiols are first blocked by MMTS. SNO-Cys residues are then selectively released by ascorbate and labeled by thiol-reactive iodoTMT reagents. (C) BV-2 cell lysates *in vitro* *S*-nitrosylated by SNOC (200 $\mu$M) were switch-labeled by iodoTMT-126. This sample exhibited strong signals on the anti-TMT immunoblot, whereas controls omitting SNOC and/or ascorbate displayed much lower signal levels. (D) BV-2 cell lysates exposed to SNOC (0, 10, 50, 100, 200 $\mu$M) were switch-labeled by iodoTMT-126. As the concentration of SNOC increased, more SNO-proteins were detected on the anti-TMT immunoblot.

## Optimization of SNO-Peptide Enrichment for the ISA Method

ISA provides a simple workflow (Figure 2A). The protocol allows both SNO-protein quantification and SNO-Cys site-mapping. Furthermore, up to six different protein samples can be simultaneously analyzed with iodoTMTsixplex reagents, iodoTMT126−131. After individually labeling of protein samples with iodoTMTsixplex reagents as shown in Figure 1B, samples are combined before trypsin digestion (Figure 2A). Since the labeling of Cys thiols by iodoTMT reagents is irreversible, reduction with DTT and alkylation with iodoacetamide are possible for more efficient digestion than that of the reversible thiol reactions. Digested peptides are then subjected to enrichment with anti-TMT antibody resin following the protocol described in Materials and Methods. Because of the low abundance of SNO-proteins and SNO-Cys modifications, it is essential to enrich the iodoTMT-labeled peptides before MS analysis. During LC−MS/MS analysis of enriched peptides, SNO-Cys are identified by the site of iodoTMT labeling and quantified based on ratios of the iodoTMTsixplex reporter ions.

A unique feature of the ISA workflow is the use of an immobilized anti-TMT resin for labeled peptide enrichment. Since an iodoTMT reagent is used to label peptides in the switch assay instead of a biotinylation reagent, endogenously biotinylated proteins are not pulled down during enrichment, resulting in improved specificity of detecting SNO-proteins. Previously, an acidic elution buffer [50% (v/v) ACN/0.4% (v/v) TFA; EB1] was used to elute TMT-labeled peptides from the anti-TMT resin after enrichment.[8,18] However, this buffer

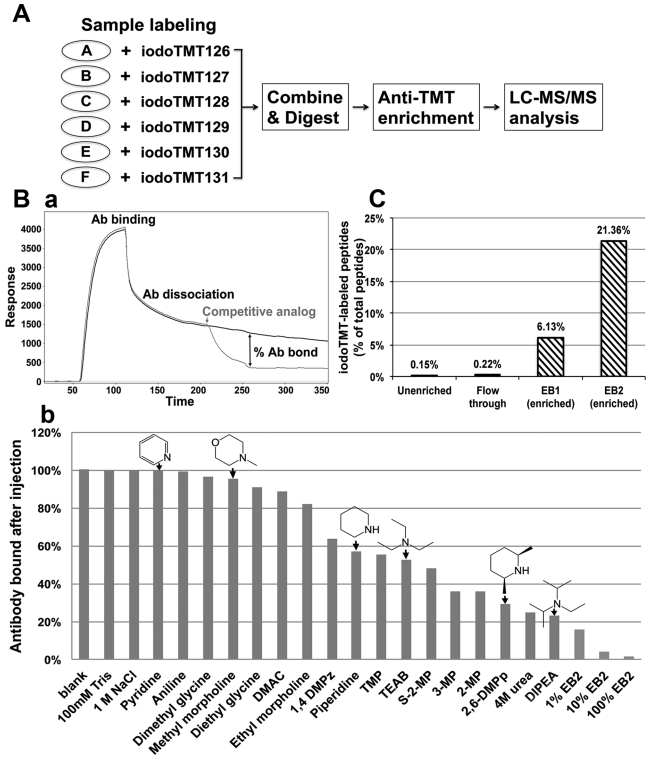


**Figure 2.** Optimization of SNO-peptide enrichment for the ISA method. (A) Workflow for ISA. Up to six protein samples can be analyzed by ISA simultaneously. After switch labeling with iodoTMTsixplex reagents as shown in Figure 1B, the six samples are combined for in-solution trypsin digestion and peptide enrichment with anti-TMT resin. The enriched peptides are analyzed by LC−MS/MS for SNO-Cys site identification and quantification based on iodoTMT reporter ions. (B) Anti-TMT antibody competitive elution using BIACORE system. (a) Surface plasmon resonance binding curve of anti-TMT binding to TMT-derivatized Biacore chip with (gray line) and without (black line) addition of a competitive TMT analogue compound. Ab, antibody. (b) Graph of competitive TMT analogue compounds screened using surface plasmon resonance. Binding data is normalized to mock injections and TMT antibody off rate steady state kinetics at 10 mM concentration of the testing compounds in 500 mM TEAB buffer, pH 8.5. DMAC, dimethylacetamide; DMPz, dimethylpiperizine, TMP, tetramethylpiperidine, MP, methylpiperidine, DMPp, 2,6-DMPp, DIPEA, diisopropylethylamine. (C) Comparison of acidic elution buffer EB1 and competitive elution buffer EB2 for enrichment of iodoTMT-labeled SNO-peptides. BV-2 cell lysates treated or untreated with SNOC (200 $\mu$M) were processed following the ISA workflow. LC−MS/MS analysis shows that iodoTMT-labeled peptides account for 0.15%, 0.22%, 6.13%, and 21.36% of total peptides in the unenriched, flow through, enriched by EB1 elution, and enriched by EB2 elution, respectively.

can also elute a certain amount of nonspecific binding peptides along with the specific TMT-labeled peptides. In order to further improve the specificity of the peptide enrichment while retaining the efficiency of the anti-TMT affinity precipitation, a new elution buffer containing a TMT structural analogue that could specifically compete for TMT-labeled peptide binding was developed. We screened a series of compounds representing various structural motifs of the TMT tag for testing anti-TMT binding affinity using a BIACORE competition assay (Figure 2B, a). We found that structural analogues of the mass tag reporter region had the greatest ability to compete for anti-TMT antibody binding (Figure 2B, b). Comparing the original acidic elution buffer EB1 with the newly developed


dx.doi.org/10.1021/pr401179v | *J. Proteome Res.* 2014, 13, 3200−3211

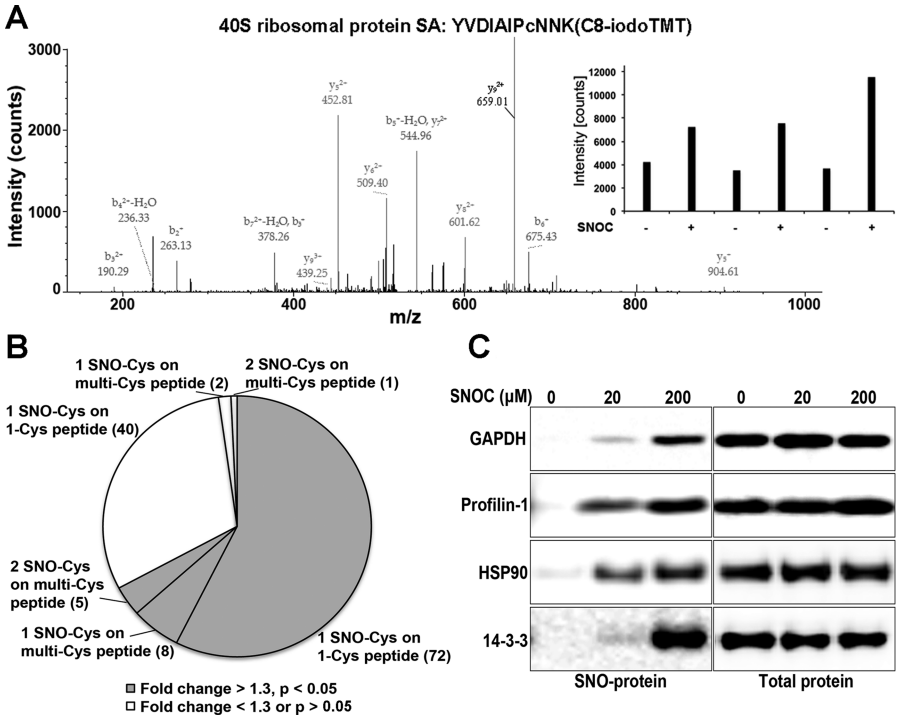


**Figure 3.** Quantitative analysis of protein *S*-nitrosylation *in vitro* using ISA. (A) BV-2 cell lysates treated or untreated with SNOC (200 $\mu$M) were analyzed by the ISA method ($n$ = 5). The MS spectrum (left) and quantification information (right) of an example peptide are shown. The coefficients of variation (CV) are 10% and 27% for the three replicates of untreated and SNOC-treated samples, respectively. (B) In total, we identified 90 SNO-Cys sites on 85 unique peptides exhibiting significant *S*-nitrosylation level changes (gray) and 44 sites on 43 peptides showing low response to SNOC treatment (white). Among the 90 significantly altered SNO-Cys sites, 8 multiple Cys-containing peptides (multi-Cys peptides) have only 1 site specifically *S*-nitrosylated; 5 multi-Cys peptides have 2 sites modified by *S*-nitrosylation; and the remaining SNO-Cys sites were identified in 72 peptides containing a single Cys (1-Cys peptides). (C) Four SNO-proteins identified by ISA were selected for validation with the BST method. Proteins in BV-2 cell lysates were *in vitro* *S*-nitrosylated by SNOC exposure (0, 20, or 200 $\mu$M) and then switch-labeled by biotin-HPDP. After pull-down with avidin, immunoblotting with individual antibodies confirmed these proteins were *S*-nitrosylated in a dose-dependent manner (left). Total proteins collected before pull-down are shown as loading controls (right).

competitive elution buffer (10 mM 2,6-DMPp/500 mM TEAB, pH 8.5; EB2) for enrichment of the iodoTMT-labeled SNO-peptides revealed a significant increase in labeled peptide percentage of total identified peptides from 6.13% to 21.36% (Figure 2C). These data show that EB2 works more effectively than that of EB1 and was therefore used in ISA for subsequent studies.

## Quantitative Analysis of Protein *S*-Nitrosylation in Vitro Using ISA

To demonstrate the efficiency of the ISA method, triplicates of untreated and SNOC (200 $\mu$M)-treated BV-2 microglial cell lysates were analyzed by ISA. Figure 3A shows a representative MS/MS spectrum of an identified SNO-peptide (left; peptide sequence: YVDIAIPcNNK; protein reference: 40S ribosomal protein SA; SNO-Cys modification site: C8). The quantification of this peptide is shown as well (Figure 3A, right). In total, 134 SNO-Cys sites were identified, and they were detected in all of the three replicates. Ninety of them from 68 proteins showed significant changes in *S*-nitrosylation level (fold change >1.3, $p < 0.05$) when comparing between untreated and SNOC-treated samples (Supplemental Table S1, Supporting Information). For the SNO-peptides significantly altered by SNOC, we were able to distinguish the modification site on eight peptides containing two Cys residues (Figure 3B and highlighted in green in Supplemental Table S1); and we also found five peptides with two or more SNO-Cys modifications per peptide (Figure 3B and highlighted in red in Supplemental Table S1). Four of the identified proteins were labeled by conventional method BST to validate these LC–MS/MS results (Figure 3C). Overall, these results show the capability of ISA for SNO-Cys site localization and quantification in multigroup samples.

## Analysis of Protein *S*-Nitrosylation in LPS-Stimulated BV-2 Cells by ISA

To assess the ability of ISA to investigate protein *S*-nitrosylation *in vivo*, we used the method to detect *S*-nitrosylation in a neuroinflammatory model using BV-2 microglial cells stimulated with LPS. Microglia are innate immune active cells in the brain and are associated with inflammatory responses to brain injury and neurological diseases such as Alzheimer's disease, Parkinson's disease, and stroke.[19−22] These cells have been shown to respond to the endotoxin LPS to induce protein *S*-nitrosylation.[9,23−25]

After BV-2 cells were exposed to LPS (100 ng/mL) for 16 h, the NO concentration in the cell culture medium significantly increased (Figure 4A, left), and no significant cell death was observed by the MTT assay (Figure 4A, right). Biological triplicate LPS-treated and untreated BV-2 cells were then lysed in HENTS buffer, and equal amounts of the lysates were labeled by iodoTMTsixplex reagents (126, 128, and 130 for LPS-treated samples; 127, 129, and 131 for untreated samples). After anti-TMT enrichment, the percentage of iodoTMT-labeled peptides increased from 0.1% to 35.1% of the total peptides (data not shown).


dx.doi.org/10.1021/pr401179v | *J. Proteome Res.* 2014, 13, 3200−3211

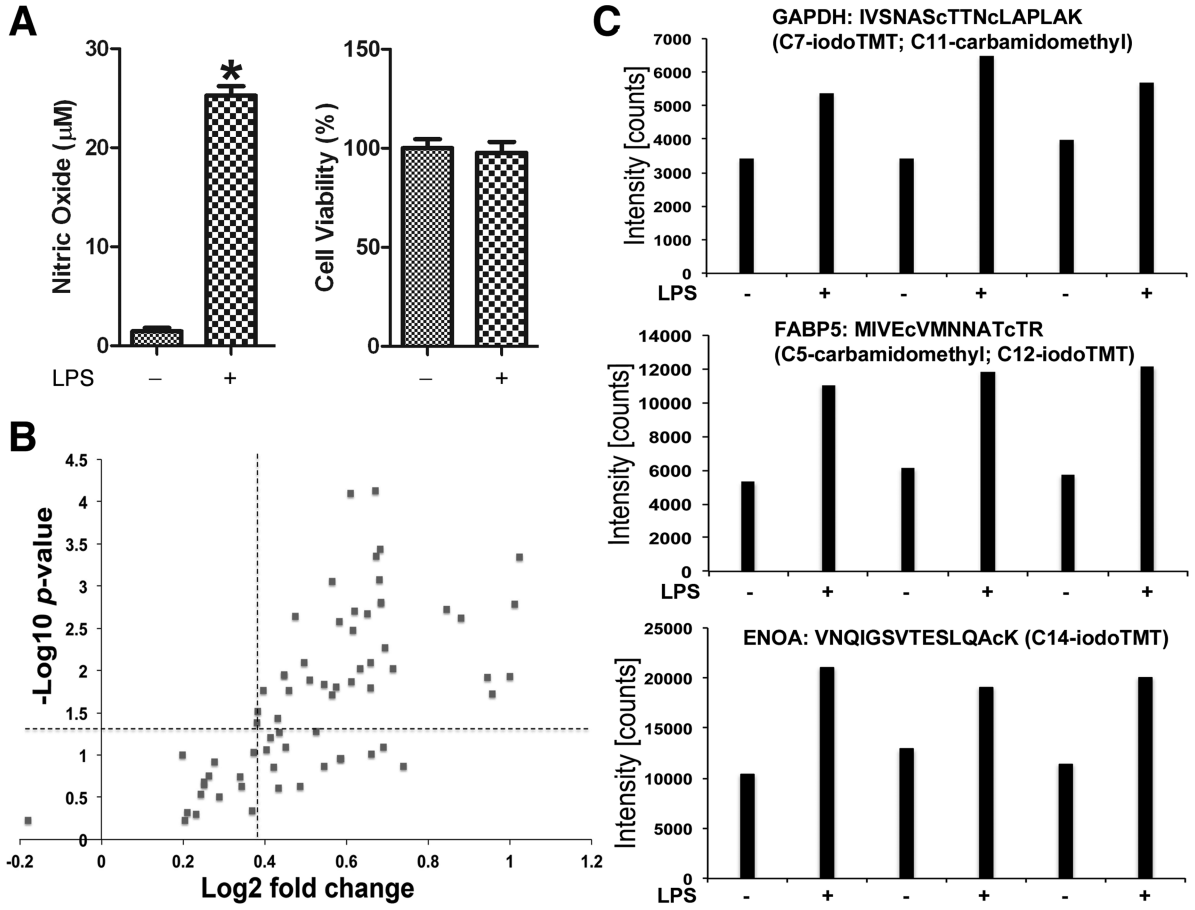


**Figure 4.** Analysis of protein *S*-nitrosylation in LPS-stimulated BV-2 microglial cells by ISA. (A) BV-2 cells were exposed to 100 ng/mL LPS for 16 h. NO production significantly increased after LPS-exposure as indicated by Griess assay (left). *, $p < 0.05$ vs untreated. Compared to the untreated sample, LPS treatment caused 2.4% cell death, which is not a significant change (MTT assay; right). (B) Untreated and LPS-treated samples were analyzed by ISA ($n = 3$). A total of 101 unique SNO-Cys sites were identified, of which 38 on 36 unique peptides showed significant differences (fold change >1.3, $p < 0.05$) in *S*-nitrosylation level between untreated and LPS-treated samples. To globally visualize the data set, a scatter plot was used to depict each of the SNO-Cys sites as a point, plotting the log2 fold change against −log10 *p*-value. The horizontal dashed line demarcates $p = 0.05$, and the vertical dashed line demarcates a 1.3-fold change. (C) The quantification information of three representative SNO-peptides is presented: IVSNAScTTNcLAPLAK from protein GAPDH [CV (untreated) = 9%, CV (LPS) = 10%], MIVEcVMNNATcTR from protein FABP5 [CV (untreated) = 7%, CV (LPS) = 5%], and VNQIGSVTESLQAcK from protein ENOA [CV (untreated) = 11%, CV (LPS) = 5%].

A total of 101 unique SNO-Cys sites were identified, and the site overlap among the three replicates is shown as Supplemental Figure S2, Supporting Information. To globally visualize the data set, log2 fold change of each SNO-Cys was plotted against −log10 *p*-value (Figure 4B). Sixty-three SNO-Cys on 60 peptides showed low response to LPS stimulation, while *S*-nitrosylation levels of 38 SNO-Cys sites on 36 peptides corresponding to 30 proteins were significantly up-regulated (fold change > 1.3, $p < 0.05$; Supplemental Table S2, Supporting Information). Among them, two peptides were detected with two SNO-Cys sites (highlighted in red in Supplemental Table S2), and four peptides were identified with one SNO-Cys and another Cys residue with a different modification (highlighted in green in Supplemental Table S2).

Figure 4C shows the relative quantification of three example peptides that responded to LPS treatment. Peptide IVSNAScTTNcLAPLAK from protein GAPDH contains one Cys residue at C7 with an iodoTMT modification and another Cys residue at C11 with carbamidomethyl modification introduced during peptide alkylation by iodoacetamide before trypsin digestion (Figure 4C, top). Peptide MIVEcVMNNATcTR from protein FABP5 has two Cys residues at C5 and C12, both of which can be *S*-nitrosylated but not simultaneously (Figure 4C, middle). We present here a peptide where C12 was *S*-nitrosylated and C5 alkylated by carbamidomethyl. ENOA peptide VNQIGSVTESLQAcK contains only one Cys, which was *S*-nitrosylated (Figure 4C, bottom). The MS/MS spectra of these three peptides are provided in Supplemental Figure S3. These results indicate that ISA is able to map SNO-Cys sites even on peptides containing more than one Cys residue and illustrates that this method is efficient in quantitative analysis of protein *S*-nitrosylation under pathophysiological conditions.

## Effect of SAC on LPS-Induced *S*-Nitrosylation in BV-2 Cells

To demonstrate the application of ISA for comprehensive *in vivo* studies and to examine the multimodal action of botanical compounds as preventive medicine, we further investigated the effect of SAC on *S*-nitrosylation in LPS-stimulated BV-2 microglial cells. As the most abundant organosulfur compound in AGE, SAC has been reported to act as an antioxidant and show protective effects in many experimental paradigms of neurodegenerative diseases including ischemic and traumatic brain injury, Alzheimer and Parkinson's disease.[26] Since activation of microglia has been implicated in neuroinflammation underlying neurodegenerative diseases, we anticipate that


dx.doi.org/10.1021/pr401179v | *J. Proteome Res.* 2014, 13, 3200−3211

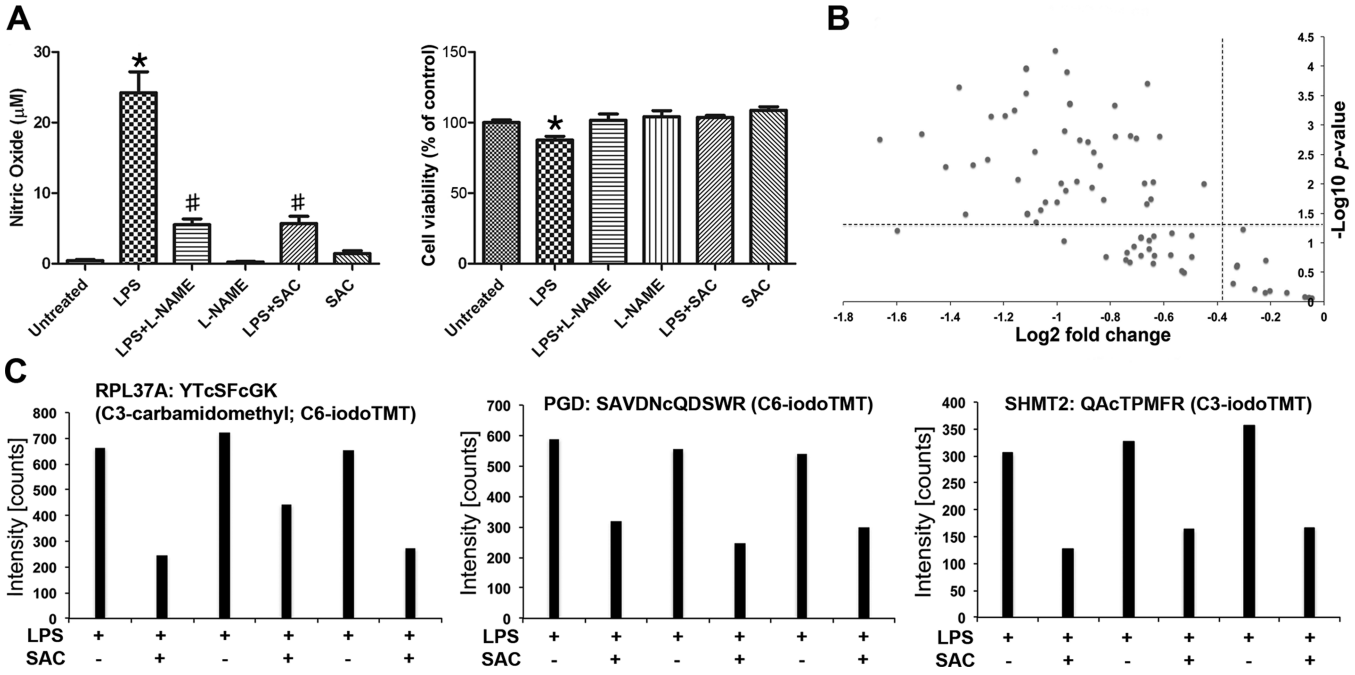


**Figure 5.** Effect of SAC on LPS-induced *S*-nitrosylation in BV-2 cells. (A) A Griess assay (left) showed that NO production in BV-2 cells induced by LPS was significantly inhibited by SAC (5 mM) treatment as well as L-NAME (0.5 mM), a known NO synthase inhibitor. *, $p < 0.05$ vs untreated; #, $p < 0.05$ vs LPS. SAC or L-NAME alone has no significantly effect on NO production. Results of MTT assay (right) indicated LPS treatment caused about 12.5% cell death; however, the addition of SAC or L-NAME did not significantly affect the cell viability. (B) We identified 115 SNO-Cys sites with 46 of them differentially *S*-nitrosylated (fold change > 1.3, $p < 0.05$) responding to SAC treatment in LPS-stimulated BV-2 cells ($n = 3$). The identified SNO-Cys sites are indicated as dots in a graph generated by plotting log2 fold change against −log10 *p*-value. The horizontal dashed line is drawn at $p = 0.05$, and the vertical dashed line is drawn at fold change = −1.3. (C) The quantitative results of three peptides YTcSFcGK [CV (LPS) = 6%, CV (LPS + SAC) = 33%], SAVDNcQDSWR [CV (LPS) = 4%, CV (LPS + SAC) = 13%], and QAcTPMFR [CV (LPS) = 8%, CV (LPS + SAC) = 15%] are given as examples.

studying the effect of SAC on protein *S*-nitrosylation in activated microglial cells would provide insights into the underlying mechanism(s) of SAC for the attenuation of excessive neuroinflammation and prevention of neurodegenerative diseases.

In this study, BV-2 cells were exposed to LPS in the presence or absence of SAC (5 mM) or L-NAME (0.5 mM), a known inhibitor of NO synthases. Our data showed that SAC significantly inhibited NO production induced by LPS but had no apparent toxicity to the cells (Figure 5A). This result is in line with a previous report showing that SAC inhibited NO production in LPS/cytokine-stimulated macrophages.[27] ISA analysis with the biological triplicate LPS-treated and LPS + SAC-treated samples identified 115 SNO-Cys sites on 110 peptides. The modification site overlap of the three replicates is shown as Supplemental Figure S4, Supporting Information. The identified SNO-Cys sites were visualized as points in a scatter plot generated by plotting log2 fold change against −log10 *p*-value (Figure 5B). A total of 46 SNO-Cys sites on 46 proteins displayed significant changes in *S*-nitrosylation levels (fold change >1.3, $p < 0.05$; Supplemental Table S3, Supporting Information). About 70% of the 46 SNO-Cys sites have been previously identified in other studies (data not shown). Figure 5C shows relative quantification of three representative iodoTMT-labeled peptides whose *S*-nitrosylation level was down-regulated upon SAC treatment.

## Pathways and Functional Analysis

In this study, we identified 68, 30, and 46 SNO-proteins that were differentially *S*-nitrosylated (fold change > 1.3, $p < 0.05$) responding to SNOC, LPS, and LPS + SAC treatments in BV-2 cells, respectively (Figure 6A). There were 14 SNO-proteins shared by SNOC- and LPS-treated samples, suggesting common and distinct signaling pathways were triggered by these two treatments. Twelve common SNO-proteins were found between LPS and LPS + SAC treatments (Figure 6A), indicating SAC partially attenuated the effect of LPS on protein *S*-nitrosylation but also had its own distinct targets. Nineteen out of 46 SNO-proteins responding to LPS + SAC-treatment were in common with the SNOC-treatment. The six SNO-proteins shared by all of the three groups include LCP1, PKM2, SLC25A5, CFL1, ENOA, and LDHA.

In order to learn more about the molecular mechanisms of NO signaling under microglial activation and of SAC to modulate LPS-induced *S*-nitrosylation in BV-2 microglial cells, we conducted functional annotation and pathway analysis of the SNO-proteins identified. IPA analysis shows the 68 SNO-proteins significantly altered by SNOC treatment are mainly associated with neurological disease, immunological disease, and inflammatory disease, while the 30 SNO-proteins in response to LPS-stimulation are mostly involved in immunological disease and inflammatory disease/response (data not shown). Other functional annotation results for SNOC and LPS treatments, including molecular and cellular functions (Supplemental Tables S4 and S5), subcellular locations, and top canonical pathways (Supplemental Figures S5 and S6) are shown in Supporting Information.

Specific effects of SAC were assessed using an in-house MULTICOM-PDCN analysis.[17] The results of this analysis shows that the 46 SNO-proteins modulated by SAC are mainly located in the cytoplasm and the nucleus (Figure 6B), and they


dx.doi.org/10.1021/pr401179v | J. Proteome Res. 2014, 13, 3200−3211

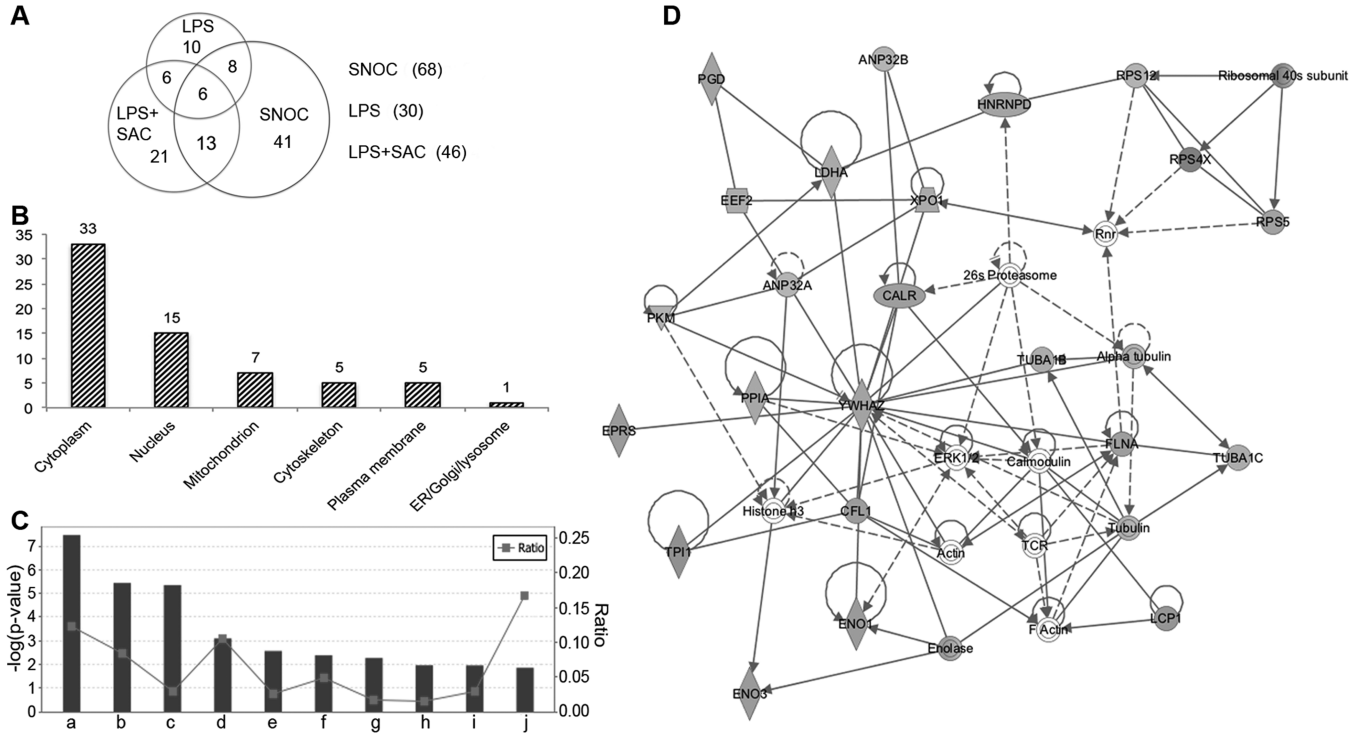


**Figure 6.** Pathway and functional annotation. (A) The overlaps between the three subsets of SNO-proteins identified from different treatment conditions in this study. (B) Subcellular location of the 46 SNO-proteins responding to SAC treatment in LPS-stimulated BV-2 cells. (C) Top 10 IPA canonical pathways targeted by SAC in LPS-stimulated BV-2 cells are presented: (a), glycolysis I; (b), gluconeogenesis I; (c), EIF2 signaling; (d), sucrose degradation; (e), 14-3-3-mediated signaling; (f), TCA cycle II (eukaryotic); (g), regulation of eIF4 and p90S6K; (h), mTOR signaling; (i), remodeling of epithelial adherent junctions; (j), glycine biosynthesis I. These pathways were ranked according to their −log (*p*-value) (black bars). A ratio (gray square) indicates the number of identified SNO-proteins found in each pathway over the total number of proteins in that pathway. (D) The top protein network associated with SAC-treatment in LPS-stimulated BV-2 cells functions in neurological disease as predicted by IPA. Twenty-seven identified SNO-proteins are involved in this network and displayed in gray. The color intensity indicates the degree of down-regulation of protein *S*-nitrosylation. Solid lines in the network imply direct interactions between proteins, and dashed lines indicate indirect interactions. Geometric shapes represent various general functional protein groups (diamond for enzyme, oval for transcription regulator, trapezoid for transporter, inverted triangle for kinase, double circle for complex/group, and circle for others). Proteins in white shapes are not part of our data set but have relationships with our proteins in the network.

are involved in diverse molecular and cellular functions including carbohydrate metabolism, cellular assembly and organization, cellular function and maintenance, molecular transport, and RNA trafficking as predicted by IPA (Table 1).

**Table 1. Molecular and Cellular Functional Annotation of the SNO-Proteins Modulated by SAC in LPS-Stimulated BV-2 Microglial Cells**

| name | *p*-value | no. molecules |
|---|---|---|
| carbohydrate metabolism | $1.09 \times 10^{-06}$ to $3.68 \times 10^{-02}$ | 10 |
| cellular assembly and organization | $2.86 \times 10^{-06}$ to $4.80 \times 10^{-02}$ | 15 |
| cellular function and maintenance | $2.86 \times 10^{-06}$ to $4.80 \times 10^{-02}$ | 14 |
| molecular transport | $5.08 \times 10^{-06}$ to $4.35 \times 10^{-02}$ | 19 |
| RNA trafficking | $5.08 \times 10^{-06}$ to $7.00 \times 10^{-03}$ | 4 |

Top canonical pathways in which these proteins participate include glycolysis I, gluconeogenesis I, EIF2 signaling, sucrose degradation, 14-3-3-mediated signaling, TCA cycle II (eukaryotic), regulation of eIF4 and p90S6K, mTOR signaling, remodeling of epithelial adherent junctions, and glycine biosynthesis I (Figure 6C). Moreover, SAC mediated a protein−protein interaction network that functions in neurological disease (Figure 6D). Twenty-seven out of the identified 46 SNO-proteins are involved in this network. These findings illustrate that SAC exhibits multimodal action on protein *S*-nitrosylation under microglial activation, which may further contribute to the reversing effects in neurological diseases.

## ■ DISCUSSION

*S*-Nitrosylation is regarded as a major mechanism for NO bioactivity[1] with participation in cellular processes, including vasodilation, neurotransmission, apoptosis, cellular trafficking, and cell cycle regulation.[28,29] To facilitate efficient investigation of *S*-nitrosylation under physiological and pathophysiological conditions, we have developed a novel MS-based ISA method based on the conventional BST assay for the detection, identification, and multiplex quantification of SNO-Cys residues. We demonstrated in both *in vitro* and *in vivo* studies under physiological conditions that ISA is an effective tool for investigation of protein *S*-nitrosylation with several unique features: (i) irreversible labeling of SNO-Cys residues for specific MS detection and site-mapping; (ii) anti-TMT enrichment and competitive elution to improve efficiency of identification of SNO-peptides; and (iii) multiplex iodoTMT reagents for unbiased quantification of SNO-proteins from complex biological samples under different conditions.


dx.doi.org/10.1021/pr401179v | *J. Proteome Res.* 2014, 13, 3200−3211

There is substantial evidence indicating that *S*-nitrosylation is a highly conserved process and is precisely regulated in cells.[1,30−34] Despite the possibility of multiple Cys residues in a protein, only specific sites can be *S*-nitrosylated in response to NO signaling and subsequently regulate protein activities.[35−37] Unlike other PTMs in proteins (e.g., phosphorylation, glycosylation, and sumoylation), the linear consensus motif and structural environment that promote protein *S*-nitrosylation are currently under intensive discussion. Increasing evidence shows a consensus acid−base motif containing an acidic or basic residue flanking the SNO-Cys sites in the primary amino acid sequence or tertiary structure plays a critical role in protein *S*-nitrosylation.[38−41] Proteome-wide studies also show that hydrophobicity of flanking residues, sulfur atom exposure, and Cys relative surface accessibility are potential factors contributing to the specificity of *S*-nitrosylation.[7,41,42] Since there are multiple molecular mechanisms for protein *S*-nitrosylation, it seems that the environments surrounding modified Cys residues possess diverse features rather than a general rule that applies to all SNO-Cys sites.[40,42] In our study, we identified a total of 133 SNO-Cys sites from 105 proteins in BV-2 cells responding to different stimulations (SNOC, LPS, and LPS + SAC; Supplemental Table S6, Supporting Information). Motif analysis by the Motif-X algorithm[16] using the 133 SNO-Cys sites identified here demonstrated six consensus sequences (Supplemental Figure S7, Supporting Information). In motifs #2, #3, and #6, modified Cys residues are flanked by an acid or basic amino acid, which is in line with the previously found acid−base motif. Motifs #4 and #5 are consistent with the previously predicted motifs containing hydrophobic amino acids. The most statistically significant consensus sequence, MxxC in motif #1, has not been observed previously, suggesting that the proximal polar amino acids may also play a role in selective Cys *S*-nitrosylation.

Given the complexity, prediction of *S*-nitrosylation sites by computational approaches remains challenging. Therefore, determining the locations of SNO-Cys sites still relies on proteomic analyses to provide large informative data sets. In previously established SNOSID and SNO-RAC methods, the labeling of SNO-proteins with biotin-HPDP or thiol-reactive resin is a reversible process, and therefore the tags can be lost during peptide elution from the resin at the affinity enrichment step.[5,6] Without labeling, it is difficult to locate the SNO-Cys sites on peptides with multiple Cys residues by MS analysis. In addition, it is difficult to exclude nonspecific peptides, thus introducing false positive signals. The peptides linked to SNO-peptides by intermolecular disulfide bonds could be one of the "nonspecific" sources, but a reduction step to break the disulfide bonds in protein samples before affinity enrichment is not feasible in these methods due to their reversible nature of SNO-Cys labeling.[43] In contrast, the iodoacetyl reaction of iodoTMT reagent with *S*-nitrosothiol used in the ISA method is irreversible resulting in a stable tagging modification even under reducing environments. The iodoTMT tag on SNO-Cys easily removes the ambiguity of site assignment and excludes potential false positive signals from nonspecific peptides in MS analysis. For example, the GAPDH peptide IVSNAScTTNcLAPLAK, corresponding to residues 144−160, was previously identified by the SNOSID method as endogenous SNO-Cys-containing peptide, although the position of the Cys residue undergoing *S*-nitrosylation was unknown.[5] In this study using the ISA approach, we successfully determined Cys-150 as the *S*-nitrosylation site but not Cys-154 in response to LPS treatment (Supplemental Table S2 and Figure 4C, Supporting Information). It has been reported that *S*-nitrosylation of GAPDH at Cys-150 leads to its binding to Siah1 (an E3 ubiquitin ligase) which further initiates apoptotic cell death.[44] On the basis of this example, unambiguous SNO-Cys site-mapping by the ISA approach can provide clues and directions for future functional analysis of SNO-proteins.

Sensitivity is an important criterion when investigating *S*-nitrosylation due to the labile nature and low abundance of this modification. However, most existing methods were assessed under very different conditions (e.g., concentrations of NO donors, cell or tissue types, or treatment conditions), resulting in difficulty in comparing sensitivity. Particularly, high doses of NO donors, beyond the range of physiological NO concentrations, were used in previous proteomics investigations. For instance, *S*-alkylating labeling strategy determined 586 SNO-Cys sites of 384 SNO-proteins from 1 mM *S*-nitroso-*N*-acetylpenicillamine/L-cysteine-treated mouse MS-1 endothelial cells,[7] and SNO-RAC identified 396 SNO-peptides using 500 $\mu$M SNOC treatment in HEK293 cells.[6] Even though a large number of SNO-proteins were identified, the biological relevance of these data and the sensitivities of these methods under *in vivo* conditions remain uncertain. Methods using physiological or pathological conditions to induce *S*-nitrosylation have previously identified up to 90 SNO-Cys sites.[5,8,18,45,46] In particular, a recent report using a sequential iodoTMT switch strategy to monitor multiple Cys modifications identified 13 SNO-Cys on 12 proteins exhibiting significant level changes in *S*-nitrosoglutathione-treated heart myoblast H9c2 cells under hypoxia conditions.[18] With similar experimental conditions, we identified 90, 38, and 46 SNO-Cys sites significantly altered by SNOC, LPS, and LPS + SAC treatments in BV-2 microglial cells, respectively. The good sensitivity of ISA results from its robust workflow with irreversible iodoTMT labeling for investigation of protein *S*-nitrosylation only and the use of competitive elution for efficient anti-TMT peptide enrichment. As shown in Figure 2C, the new volatile competitive elution buffer containing a TMT analogue (2,6-DMPp) significantly increased the percentage of the iodoTMT-labeled peptides in total identified peptides (21.36%) compared to that eluted by the nonselective acidic elution buffer (6.13%), which was used in previous studies.[8,18]

Multiplex quantification using LC−MS/MS is a powerful method for simultaneous analysis of samples from biological replicates, time courses, or different experimental conditions such as healthy versus disease or various drug treatments. Previously, MS quantification of *S*-nitrosylation has been accomplished using isotope-coded affinity tags (ICAT) labeling,[43,47] *S*-nitrosothiol capture (SNOCAP) reagents,[48] isobaric tag for relative and absolute quantitation (iTRAQ)-coupled SNO-capture techniques,[6] or cysTMT switch labeling.[8] ICAT and SNOCAP are stable isotope labeling methods for comparing relative peptide abundance at the MS level but are limited to the analysis of two samples at a time. Moreover, the quantification of peptide ratios using MS peak intensities may be unreliable due to the shift of elution time between the light and heavy labeled counterparts on the RP-LC separation by ICAT and SNOCAP.[49] In contrast, isobaric tags with the identical mass and chemical structures (e.g., iTRAQ and TMT) allow for multiplexing up to 8 or 10 samples in a single LC−MS/MS analysis. Amine-reactive iTRAQ tags have been used for labeling SNO-peptides, but as there is no mass signature on SNO-Cys, the SNO-RAC workflow is unable to localize SNO-

Cys sites despite MS quantification of the enriched peptides.[6] Utilizing isobaric cysTMTsixplex reagents in the cysTMT switch assay achieves both site-mapping and multiplex quantification.[8] However, the output of this method is relatively low for cell-based study, as only 25 SNO-Cys sites were detected from SNOC (200 $\mu$M)-treated cells. Since cysTMT labeling of SNO-proteins is reversible, it is not compatible with reduction/alkylation, which is required for complete protein denaturation before trypsin digestion. This may result in incomplete digestion in complicated protein samples therefore hindering the efficiency of MS detection. Unlike cysTMT, the iodoTMT reagents irreversibly label Cys thiols for improved labeling of SNO-proteins. Coupled with the improved competitive elution buffer for anti-TMT enrichment, the ISA workflow allows for multiplex *S*-nitrosylation sample analysis with high efficiency and specificity.

Emerging evidence indicates that protein *S*-nitrosylation exerts critical roles in a variety of cellular processes by regulating protein folding, ubiquitination, mitochondrial dynamics, and signal transduction.[3,50−53] Many neurodegenerative diseases involve nitrosative stress and proinflammatory responses including protein *S*-nitrosylation with activation of microglial cells.[19,54,55] Our investigation of the *S*-nitrosylation proteome using ISA in LPS-stimulated BV-2 cells provided insights into the NO signaling pathways under microglial activation and shed light on possible molecular mechanisms contributing to neurological diseases. IPA results showed that several mitochondrial metabolic pathways (e.g., glycolysis I, gluconeogenesis I, and TCA cycle II) are altered by *S*-nitrosylation in LPS-stimulated BV-2 microglial cells (Supplemental Figure S6, Supporting Information). These results are consistent with a recent report in which a number of enzymes that regulate these metabolic pathways were found to be *S*-nitrosylated in different mouse organs.[56] There are also other studies showing that glycolysis was increased in LPS-induced BV-2 cells,[57] and monocyte-derived inflammatory dendritic cells committed to glycolysis to maintain ATP levels when oxidative phosphorylation was inhibited by NO.[58] It is possible that *S*-nitrosylation of the enzymes in glycolysis and other mitochondrial metabolic pathways identified here are involved in the regulation of these pathways during inflammatory response.

SAC is a botanical compound extracted from AGE that possesses antioxidant properties.[26] Administration of SAC to cells before LPS induction of *S*-nitrosylation was able to restore the effect of LPS on glycolysis I and gluconeogenesis I (Figure 6C), suggesting a protective effect for SAC on mitochondrial metabolism. To our knowledge, this is the first time SAC has been linked to glycolytic/gluconeogenic metabolism regulation. Our data also showed that SAC altered protein *S*-nitrosylation in the eIF2 (eukaryotic initiation factor 2) signaling pathway, which is known to be an important pathway controlling translation initiation of cellular recovery genes in response to various stresses in eukaryotic cells and is associated with pathogenesis of neurodegenerative diseases including Alzheimer's disease.[59,60] SAC may act through eIF2 signaling as well as other neurological disease-related pathways identified here (Figure 6C), such as mTOR- and 14-3-3-mediated signaling,[61−63] to take part in nitrosative stress defense.

Collectively, our data demonstrate that the ISA method is a powerful tool to profile protein *S*-nitrosylation under physiological/pathological conditions. ISA provides a simple solution to the multiple problems existing in previous methods for *S*-nitrosylation analysis. With high specificity, high sensitivity, and site-mapping/quantification ability, ISA well meets many of the current demands for the investigation of protein *S*-nitrosylation. This approach could have broad applications in the determination and comparison of *S*-nitrosylation proteome under various conditions. It can be used to help further our understanding of molecular mechanisms for NO signaling and progression of diseases. Moreover, it may also facilitate identifying potential therapeutic targets for disease treatment and elucidating effects of drugs.

## ■ ASSOCIATED CONTENT

### Supporting Information

Supplementary figures and tables. This material is available free of charge via the Internet at http://pubs.acs.org.

## ■ AUTHOR INFORMATION

### Corresponding Author

*Address: Department of Pathology and Anatomical Sciences, University of Missouri School of Medicine, M263 Medical Science Building, One Hospital Drive, Columbia, MO 65212, USA. Tel: 573-884-3880. Fax: 573-884-4612. E-mail: guze@health.missouri.edu.

### Notes

The authors declare no competing financial interests.
[&]Deceased.

## ■ ACKNOWLEDGMENTS

This publication was made possible by funding of the 5P01ES016738-02 Missouri Consortium from the National Institute of Environmental Health Science (NIEHS) and the Department of Pathology and Anatomical Sciences research fund at University of Missouri (to ZG), as well as by Grant Number P50AT006273 from the National Center for Complementary and Alternative Medicines (NCCAM), the Office of Dietary Supplements (ODS), and the National Cancer Institute (NCI). Its contents are solely the responsibility of the authors and do not necessarily represent the official views of the NIEHS, NCCAM, ODS, NCI, or the National Institutes of Health.

## ■ ABBREVIATIONS

ACN, acetonitrile; AGE, aged garlic extract; BCA, bicinchoninic acid; biotin-HPDP, *N*-[6-(Biotinamido)hexyl]-3′-(2′-pyridyldithio) propionamide; BST, biotin switch technique; CID, collision-induced dissociation; Cys, cysteine; 2,6-DMPp, cis-2,6-dimethylpiperidine; CV, coefficient of variation; DMEM, Dulbecco's modified Eagle's medium; FBS, fetal bovine serum; FT, Fourier transform; HCD, higher-energy collision dissociation; ICAT, isotope-coded affinity tags; IPA, Ingenuity Pathway Analysis; iodoTMT, Cys thiol-reactive iodoacetyl tandem mass tag; ISA, iodoTMT switch assay; iTRAQ, isobaric tag for relative and absolute quantitation; L-NAME, *N*-omega-nitro-L-arginine methyl ester hydrochloride; LPS, lipopolysaccharide; MMTS, *S*-methyl methanethiosulfonate; MS, mass spectrometry; LC−MS/MS, liquid chromatography−tandem MS; MTT, 3-(4,5-dimethylthiazol-2-yl)-2,5-diphenyl-2*H*-tetrazolium bromide; NO, nitric oxide; RT, room temperature; SAC, *S*-allyl cysteine; SNOCAP, *S*-nitrosothiol capture; SNORAC, *S*-nitrosothiol resin-assisted capture; SNOC, *S*-nitrosocysteine; SNO-Cys, *S*-nitrosylated cysteine; SNO-peptide, *S*-

nitrosylated peptide; SNO-protein, *S*-nitrosylated protein; SNOSID, SNO-Cys site identification; TEAB, tetraethylammonium bicarbonate; TFA, trifluoroacetic acid

## REFERENCES


(1) Hess, D. T.; Matsumoto, A.; Kim, S. O.; Marshall, H. E.; Stamler, J. S. Protein S-nitrosylation: purview and parameters. *Nat. Rev. Mol. Cell Biol.* **2005**, *6* (2), 150−166.

(2) Foster, M. W.; Hess, D. T.; Stamler, J. S. Protein S-nitrosylation in health and disease: a current perspective. *Trends Mol. Med.* **2009**, *15* (9), 391−404.

(3) Gu, Z.; Nakamura, T.; Lipton, S. A. Redox reactions induced by nitrosative stress mediate protein misfolding and mitochondrial dysfunction in neurodegenerative diseases. *Mol. Neurobiol.* **2010**, *41* (2−3), 55−72.

(4) Jaffrey, S. R.; Erdjument-Bromage, H.; Ferris, C. D.; Tempst, P.; Snyder, S. H. Protein S-nitrosylation: a physiological signal for neuronal nitric oxide. *Nat. Cell Biol.* **2001**, *3* (2), 193−7.

(5) Hao, G.; Derakhshan, B.; Shi, L.; Campagne, F.; Gross, S. S. SNOSID, a proteomic method for identification of cysteine S-nitrosylation sites in complex protein mixtures. *Proc. Natl. Acad. Sci. U.S.A.* **2006**, *103* (4), 1012−7.

(6) Forrester, M. T.; Thompson, J. W.; Foster, M. W.; Nogueira, L.; Moseley, M. A.; Stamler, J. S. Proteomic analysis of S-nitrosylation and denitrosylation by resin-assisted capture. *Nat. Biotechnol.* **2009**, *27* (6), 557−9.

(7) Chen, Y. J.; Ku, W. C.; Lin, P. Y.; Chou, H. C.; Khoo, K. H.; Chen, Y. J. S-alkylating labeling strategy for site-specific identification of the S-nitrosoproteome. *J. Proteome Res.* **2010**, *9* (12), 6417−39.

(8) Murray, C. I.; Uhrigshardt, H.; O'Meally, R. N.; Cole, R. N.; Van Eyk, J. E. Identification and quantification of S-nitrosylation by cysteine reactive tandem mass tag switch assay. *Mol. Cell. Proteomics* **2012**, *11* (2), No. M111.013441.

(9) Shen, S.; Yu, S.; Binek, J.; Chalimoniuk, M.; Zhang, X.; Lo, S. C.; Hannink, M.; Wu, J.; Fritsche, K.; Donato, R.; Sun, G. Y. Distinct signaling pathways for induction of type II NOS by IFNgamma and LPS in BV-2 microglial cells. *Neurochem. Int.* **2005**, *47* (4), 298−307.

(10) Li, N.; McLaren, J. E.; Michael, D. R.; Clement, M.; Fielding, C. A.; Ramji, D. P. ERK is integral to the IFN-gamma-mediated activation of STAT1, the expression of key genes implicated in atherosclerosis, and the uptake of modified lipoproteins by human macrophages. *J. Immunol.* **2010**, *185* (5), 3041−8.

(11) Miller, R. L.; Sun, G. Y.; Sun, A. Y. Cytotoxicity of paraquat in microglial cells: Involvement of PKCdelta- and ERK1/2-dependent NADPH oxidase. *Brain Res.* **2007**, *1167*, 129−39.

(12) Mosmann, T. Rapid colorimetric assay for cellular growth and survival: application to proliferation and cytotoxicity assays. *J. Immunol. Methods* **1983**, *65* (1−2), 55−63.

(13) Welch, B. L. The generalisation of student's problems when several different population variances are involved. *Biometrika* **1947**, *34* (1−2), 28−35.

(14) Johnson, N. L.; Kotz, S.; Balakrishnan, N. *Continuous Univariate Distributions*; Wiley: New York, 1995; Vol. 2.

(15) Becker, R. A.; Chambers, J. M.; Wilks, A. R. *The New S Language*; Wadsworth & Brooks: Pacific Grove, CA, 1988; p 1.

(16) Schwartz, D.; Gygi, S. P. An iterative statistical approach to the identification of protein phosphorylation motifs from large-scale data sets. *Nat. Biotechnol.* **2005**, *23* (11), 1391−8.

(17) Wang, Z.; Eickholt, J.; Cheng, J. MULTICOM: a multi-level combination approach to protein structure prediction and its assessments in CASP8. *Bioinformatics* **2010**, *26* (7), 882−8.

(18) Pan, K. T.; Chen, Y. Y.; Pu, T. H.; Chao, Y. S.; Yang, C. Y.; Bomgarden, R. D.; Rogers, J. C.; Meng, T. C.; Khoo, K. H. Mass spectrometry-based quantitative proteomics for dissecting multiplexed redox cysteine modifications in nitric oxide-protected cardiomyocyte under hypoxia. *Antioxid. Redox Signal.* **2013**, *20*, 1365−1381.

(19) Benveniste, E. N.; Nguyen, V. T.; O'Keefe, G. M. Immunological aspects of microglia: relevance to Alzheimer's disease. *Neurochem. Int.* **2001**, *39* (5−6), 381−91.

(20) Yenari, M. A.; Kauppinen, T. M.; Swanson, R. A. Microglial activation in stroke: therapeutic targets. *Neurotherapeutics* **2010**, *7* (4), 378−91.

(21) Van Eldik, L. J.; Thompson, W. L.; Ralay Ranaivo, H.; Behanna, H. A.; Martin Watterson, D. Glia proinflammatory cytokine upregulation as a therapeutic target for neurodegenerative diseases: function-based and target-based discovery approaches. *Int. Rev. Neurobiol.* **2007**, *82*, 277−96.

(22) Miller, D. W.; Cookson, M. R.; Dickson, D. W. Glial cell inclusions and the pathogenesis of neurodegenerative diseases. *Neuron Glia Biol.* **2004**, *1* (1), 13−21.

(23) Lu, X.; Ma, L.; Ruan, L.; Kong, Y.; Mou, H.; Zhang, Z.; Wang, Z.; Wang, J. M.; Le, Y. Resveratrol differentially modulates inflammatory responses of microglia and astrocytes. *J. Neuroinflammation* **2010**, *7*, 46.

(24) Possel, H.; Noack, H.; Putzke, J.; Wolf, G.; Sies, H. Selective upregulation of inducible nitric oxide synthase (iNOS) by lipopolysaccharide (LPS) and cytokines in microglia: in vitro and in vivo studies. *Glia* **2000**, *32* (1), 51−9.

(25) Thampithak, A.; Jaisin, Y.; Meesarapee, B.; Chongthammakun, S.; Piyachaturawat, P.; Govitrapong, P.; Supavilai, P.; Sanvarinda, Y. Transcriptional regulation of iNOS and COX-2 by a novel compound from Curcuma comosa in lipopolysaccharide-induced microglial activation. *Neurosci. Lett.* **2009**, *462* (2), 171−5.

(26) Colin-Gonzalez, A. L.; Santana, R. A.; Silva-Islas, C. A.; Chanez-Cardenas, M. E.; Santamaria, A.; Maldonado, P. D. The antioxidant mechanisms underlying the aged garlic extract- and S-allylcysteine-induced protection. *Oxid. Med. Cell Longev.* **2012**, *2012*, 907162.

(27) Kim, K. M.; Chun, S. B.; Koo, M. S.; Choi, W. J.; Kim, T. W.; Kwon, Y. G.; Chung, H. T.; Billiar, T. R.; Kim, Y. M. Differential regulation of NO availability from macrophages and endothelial cells by the garlic component S-allyl cysteine. *Free Radic. Biol. Med.* **2001**, *30* (7), 747−56.

(28) Greco, T. M.; Hodara, R.; Parastatidis, I.; Heijnen, H. F.; Dennehy, M. K.; Liebler, D. C.; Ischiropoulos, H. Identification of S-nitrosylation motifs by site-specific mapping of the S-nitrosocysteine proteome in human vascular smooth muscle cells. *Proc. Natl. Acad. Sci. U.S.A.* **2006**, *103* (19), 7420−5.

(29) Seth, D.; Stamler, J. S. The SNO-proteome: causation and classifications. *Curr. Opin. Chem. Biol.* **2011**, *15* (1), 129−136.

(30) Stamler, J. S.; Lamas, S.; Fang, F. C. Nitrosylation: the prototypic redox-based signaling mechanism. *Cell* **2001**, *106* (6), 675−83.

(31) Boehning, D.; Snyder, S. H. Novel neural modulators. *Annu. Rev. Neurosci.* **2003**, *26*, 105−31.

(32) Barouch, L. A.; Harrison, R. W.; Skaf, M. W.; Rosas, G. O.; Cappola, T. P.; Kobeissi, Z. A.; Hobai, I. A.; Lemmon, C. A.; Burnett, A. L.; O'Rourke, B.; Rodriguez, E. R.; Huang, P. L.; Lima, J. A.; Berkowitz, D. E.; Hare, J. M. Nitric oxide regulates the heart by spatial confinement of nitric oxide synthase isoforms. *Nature* **2002**, *416* (6878), 337−9.

(33) Lane, P.; Hao, G.; Gross, S. S. S-nitrosylation is emerging as a specific and fundamental posttranslational protein modification: head-to-head comparison with O-phosphorylation. *Sci. STKE* **2001**, *2001* (86), No. re1.

(34) Foster, M. W.; McMahon, T. J.; Stamler, J. S. S-nitrosylation in health and disease. *Trends Mol. Med.* **2003**, *9* (4), 160−8.

(35) Fang, J.; Nakamura, T.; Cho, D. H.; Gu, Z.; Lipton, S. A. S-nitrosylation of peroxiredoxin 2 promotes oxidative stress-induced neuronal cell death in Parkinson's disease. *Proc. Natl. Acad. Sci. U.S.A.* **2007**, *104* (47), 18742−7.

(36) Selvakumar, B.; Huganir, R. L.; Snyder, S. H. S-nitrosylation of stargazin regulates surface expression of AMPA-glutamate neurotransmitter receptors. *Proc. Natl. Acad. Sci. U.S.A.* **2009**, *106* (38), 16440−5.

(37) Rahman, M. A.; Senga, T.; Ito, S.; Hyodo, T.; Hasegawa, H.; Hamaguchi, M. S-nitrosylation at cysteine 498 of c-Src tyrosine kinase regulates nitric oxide-mediated cell invasion. *J. Biol. Chem.* **2010**, *285* (6), 3806−14.
(38) Stamler, J. S.; Toone, E. J.; Lipton, S. A.; Sucher, N. J. (S)NO signals: translocation, regulation, and a consensus motif. *Neuron* **1997**, *18* (5), 691−6.
(39) Ascenzi, P.; Colasanti, M.; Persichini, T.; Muolo, M.; Polticelli, F.; Venturini, G.; Bordo, D.; Bolognesi, M. Re-evaluation of amino acid sequence and structural consensus rules for cysteine-nitric oxide reactivity. *Biol. Chem.* **2000**, *381* (7), 623−7.
(40) Doulias, P. T.; Greene, J. L.; Greco, T. M.; Tenopoulou, M.; Seeholzer, S. H.; Dunbrack, R. L.; Ischiropoulos, H. Structural profiling of endogenous S-nitrosocysteine residues reveals unique features that accommodate diverse mechanisms for protein S-nitrosylation. *Proc. Natl. Acad. Sci. U.S.A.* **2010**, *107* (39), 16958−63.
(41) Marino, S. M.; Gladyshev, V. N. Structural analysis of cysteine S-nitrosylation: a modified acid-based motif and the emerging role of trans-nitrosylation. *J. Mol. Biol.* **2010**, *395* (4), 844−59.
(42) Lee, Y. I.; Giovinazzo, D.; Kang, H. C.; Lee, Y.; Jeong, J. S.; Doulias, P. T.; Xie, Z.; Hu, J.; Ghasemi, M.; Ischiropoulos, H.; Qian, J.; Zhu, H.; Blackshaw, S.; Dawson, V. L.; Dawson, T. M. Protein microarray characterization of the S-nitrosoproteome. *Mol. Cell. Proteomics* **2014**, *13* (1), 63−72.
(43) Huang, B.; Chen, C. Detection of protein S-nitrosation using irreversible biotinylation procedures (IBP). *Free Radic. Biol. Med.* **2010**, *49* (3), 447−56.
(44) Hara, M. R.; Agrawal, N.; Kim, S. F.; Cascio, M. B.; Fujimuro, M.; Ozeki, Y.; Takahashi, M.; Cheah, J. H.; Tankou, S. K.; Hester, L. D.; Ferris, C. D.; Hayward, S. D.; Snyder, S. H.; Sawa, A. S-nitrosylated GAPDH initiates apoptotic cell death by nuclear translocation following Siah1 binding. *Nat. Cell Biol.* **2005**, *7* (7), 665−74.
(45) Murray, C. I.; Kane, L. A.; Uhrigshardt, H.; Wang, S. B.; Van Eyk, J. E. Site-mapping of in vitro S-nitrosation in cardiac mitochondria: implications for cardioprotection. *Mol. Cell. Proteomics* **2011**, *10* (3), No. M110.004721.
(46) Han, P.; Chen, C. Detergent-free biotin switch combined with liquid chromatography/tandem mass spectrometry in the analysis of S-nitrosylated proteins. *Rapid Commun. Mass Spectrom.* **2008**, *22* (8), 1137−45.
(47) Chen, Y. Y.; Chu, H. M.; Pan, K. T.; Teng, C. H.; Wang, D. L.; Wang, A. H.; Khoo, K. H.; Meng, T. C. Cysteine S-nitrosylation protects protein-tyrosine phosphatase 1B against oxidation-induced permanent inactivation. *J. Biol. Chem.* **2008**, *283* (50), 35265−72.
(48) Paige, J. S.; Xu, G.; Stancevic, B.; Jaffrey, S. R. Nitrosothiol reactivity profiling identifies S-nitrosylated proteins with unexpected stability. *Chem. Biol.* **2008**, *15* (12), 1307−16.
(49) She, Y. M.; Rosu-Myles, M.; Walrond, L.; Cyr, T. D. Quantification of protein isoforms in mesenchymal stem cells by reductive dimethylation of lysines in intact proteins. *Proteomics* **2012**, *12* (3), 369−79.
(50) Chung, K. K.; Thomas, B.; Li, X.; Pletnikova, O.; Troncoso, J. C.; Marsh, L.; Dawson, V. L.; Dawson, T. M. S-nitrosylation of parkin regulates ubiquitination and compromises parkin's protective function. *Science* **2004**, *304* (5675), 1328−31.
(51) Yao, D.; Gu, Z.; Nakamura, T.; Shi, Z. Q.; Ma, Y.; Gaston, B.; Palmer, L. A.; Rockenstein, E. M.; Zhang, Z.; Masliah, E.; Uehara, T.; Lipton, S. A. Nitrosative stress linked to sporadic Parkinson's disease: S-nitrosylation of parkin regulates its E3 ubiquitin ligase activity. *Proc. Natl. Acad. Sci. U.S.A.* **2004**, *101* (29), 10810−4.
(52) Uehara, T.; Nakamura, T.; Yao, D.; Shi, Z. Q.; Gu, Z.; Ma, Y.; Masliah, E.; Nomura, Y.; Lipton, S. A. S-nitrosylated protein-disulphide isomerase links protein misfolding to neurodegeneration. *Nature* **2006**, *441* (7092), 513−7.
(53) Cho, D. H.; Nakamura, T.; Fang, J.; Cieplak, P.; Godzik, A.; Gu, Z.; Lipton, S. A. S-nitrosylation of Drp1 mediates beta-amyloid-related mitochondrial fission and neuronal injury. *Science* **2009**, *324* (5923), 102−5.
(54) Kacimi, R.; Giffard, R. G.; Yenari, M. A. Endotoxin-activated microglia injure brain derived endothelial cells via NF-kappaB, JAK-STAT and JNK stress kinase pathways. *J. Inflamm. (London)* **2011**, *8*, 7.
(55) Olson, J. K.; Miller, S. D. Microglia initiate central nervous system innate and adaptive immune responses through multiple TLRs. *J. Immunol* **2004**, *173* (6), 3916−24.
(56) Doulias, P. T.; Tenopoulou, M.; Greene, J. L.; Raju, K.; Ischiropoulos, H. Nitric oxide regulates mitochondrial fatty acid metabolism through reversible protein S-nitrosylation. *Sci. Signal.* **2013**, *6* (256), No. rs1.
(57) Volobouéva, L. A.; Emery, J. F.; Sun, X.; Giffard, R. G. Inflammatory response of microglial BV-2 cells includes a glycolytic shift and is modulated by mitochondrial glucose-regulated protein 75/mortalin. *FEBS Lett.* **2013**, *587* (6), 756−62.
(58) Everts, B.; Amiel, E.; van der Windt, G. J.; Freitas, T. C.; Chott, R.; Yarasheski, K. E.; Pearce, E. L.; Pearce, E. J. Commitment to glycolysis sustains survival of NO-producing inflammatory dendritic cells. *Blood* **2012**, *120* (7), 1422−31.
(59) Sonenberg, N.; Hinnebusch, A. G. Regulation of translation initiation in eukaryotes: mechanisms and biological targets. *Cell* **2009**, *136* (4), 731−45.
(60) Chang, R. C.; Wong, A. K.; Ng, H. K.; Hugon, J. Phosphorylation of eukaryotic initiation factor-2alpha (eIF2alpha) is associated with neuronal degeneration in Alzheimer's disease. *Neuroreport* **2002**, *13* (18), 2429−32.
(61) Steinacker, P.; Aitken, A.; Otto, M. 14-3-3 proteins in neurodegeneration. *Semin. Cell Dev. Biol.* **2011**, *22* (7), 696−704.
(62) Foote, M.; Zhou, Y. 14-3-3 proteins in neurological disorders. *Int. J. Biochem. Mol. Biol.* **2012**, *3* (2), 152−64.
(63) Wong, M. Mammalian target of rapamycin (mTOR) pathways in neurological diseases. *Biomed. J.* **2013**, *36* (2), 40−50.